PHYSICAL REVIEW A VOLUME 26, NUMBER 2 AUGUST 1982

Energy-dependent polarization potential, dispersion-relation absorption potential, and matrix effective potential for electron-neon scattering at 10—100 eV

Devarajan Thirumalai* and Donald G. Truhlar
Department of Chemistry, University of Minnesota, Minneapolis, Minnesota 55455
(Received 4 January 1982)

We report model-potential calculations of the elastic and absorption cross sections for *e*-Ne scattering at 10, 30, 50, and 100 eV. Altogether nine different model potentials are studied; these include the variational matrix-effective-potential method, an absorption potential calculated *ab initio* from a real energy-dependent polarization potential and a dispersion relation, and two different phenomenological absorption potentials. We get good agreement with experimental results by several methods at 30—100 eV and by one method at 10 eV. The tests of the various methods establish useful trends and expectations for future work.

I. INTRODUCTION

A serious difficulty in quantum-mechanical calculations of electron-atom and electron-molecule scattering in the intermediate-energy range is the accurate representation of the dynamic effects of charge polarization during the collision. One general approach, the close-coupling method and its modifications, is to expand the system wave function in terms of eigenstates and/or pseudostates of the target. This leads to coupled-channels equations for the relative motion wave functions whose solution includes all dynamic effects that can be represented within the chosen basis.[1] For some processes, especially at low energies, the basis may be taken large enough to converge the collisional attribute of interest, e.g., a particular differential cross section at some impact energy, but for many others this is not practically possible. A second approach, the one studied here, is the use of effective potentials. In particular we consider application of effective potentials to calculate integral and differential cross sections for elastic scattering and total (elastic plus inelastic) scattering cross sections for electron-neon scattering at the intermediate energies 10—100 eV.

We consider and compare two quite different effective potential approaches to this problem. Both approaches are recent suggestions, and both take the adiabatic polarization potential (APP) as a starting point. The recent implementation of general variational techniques for calculating electron-atom and electron-molecule adiabatic polarization potentials[2—7] means that the approaches presented here may be considered as general ones, i.e., not limited to simple atoms. The first approach involves a complex-valued single-channel optical-model potential and the second involves a real-valued matrix effective potential (MEP).

Two approaches to the optical-model potential have been explored computationally by other workers: the phenomenological approach[8—12] and the eikonal optical model.[13] The optical potential may also be approximated in a nonmodel context, e.g., by many-body perturbation theory[14] or the Feshbach projection formalism.[15] The new approach explored here has been suggested only recently and so far applied only to electron-helium scattering.[16] In this approach, the real part $V^P(r,E)$ of the target-response contribution to the optical-model potential is an energy-dependent polarization potential, and the imaginary part $V^A(r,E)$ is obtained by an approximate solution[16] of the dispersion relation[17] that relates $V^P(r,E)$ to $V^A(r,E)$. In the present application the energy-dependent polarization potential (EDPP) is a model potential[18] based on the APP and a leading nonadiabatic term.[19,20]

The MEP model[18,21] is another new method. So far it has been applied only to electron-helium scattering at 12—400 eV,[18,21] electron-neon scattering at 150—700 eV,[22] and atom-vibrator collisions.[23] In the MEP method one determines the matrix potential in a set of coupled-channels equations by the requirement that it agree with the static-exchange potential in the decoupling limit and with the static-exchange-plus-APP in the adiabatic limit. In the application to electron-helium scattering,[18,21] the available APP (Refs. 24 and 25)

was determined by second-order perturbation theory so the adiabatic limit of the coupled-channel equations was taken by second-order perturbation theory. For neon the available APP is a variational one[7] so we take the adiabatic limit consistent with a variational APP. In the application to helium we considered both two and three-channel versions of the theory,[18,21] and we have also considered perturbative and variational multichannel versions in an application of the same idea to vibrational excitation in atom-molecule collisions.[23] In the present work we limit ourselves to the variational two-channel implementation.

The results of the two new approaches will be compared to each other, to new phenomenological optical-potential calculations, to previous theoretical calculations,[9,11,26–32] and to recent experimental results.[33–42]

We use Hartree atomic units in which the unit of energy is the hartree (E_h); distance, the bohr (a_0); mass, the mass of an electron; and action, $\hbar$.

II. THEORY

A. Energy-dependent polarization potential and dispersion-relation absorption potential

In the EDPP of Onda and one of the authors,[18] we begin by examining two of the leading terms in the large-r, i.e., small-perturbation, limit of the real part of the optical potential. The real part of the optical potential consists of the static-exchange part $V^{\mathrm{SE}}(r,E)$ and the rest, where the latter is the contribution due to target response and will be called $V^{P}(r,E)$. At large r the leading contributions to $V^{P}(r,E)$ may be computed in the dipole approximation. The leading term is the adiabatic dipole term $V^{\mathrm{Pa(di)}}(r)$ and the leading energy-dependent term will be called $V^{\mathrm{Pe(di)}}(r,E)$. Making the average-excitation-energy approximation, with average excitation energy ω, yields

$$V^{\mathrm{Pa(di)}}(r) \underset{r\to\infty}{\sim} -\frac{S}{\omega r^4}, \tag{1}$$

$$V^{\mathrm{Pe(di)}}(r,E) \underset{r\to\infty}{\sim} \frac{6Sk^2}{\omega^3 r^6}, \tag{2}$$

where

$$S=\sum_n{}' |z_{n1}|^2, \tag{3}$$

z_{n1} is the z component of the transition dipole matrix element between state n and the ground state ($n=1$), and the impact energy in Hartree atomic units is $E=k^2/2$ where k is the initial relative wave number. Combining (1) and (2) yields

$$V^{\mathrm{Pa(di)}}(r)+V^{\mathrm{Pe(di)}}(r,E) \underset{r\to\infty}{\sim} V^{\mathrm{Pa(di)}}(r)\left[1-\frac{6k^2}{\omega^2 r^2}\right]. \tag{4}$$

The assumption of the EDPP is that relation (4) may be generalized to the polarization potential at all r as follows:

$$V^{\mathrm{Pna}}(r,E)=V^{\mathrm{Pa}}(r)\Big/\left[1+\frac{6k^2}{\omega^2 r^2}\right] \tag{5}$$

since the right-hand side of (5) tends to the right-hand side of (4) at large r. The nonadiabatic polarization (Pna) potential of Eq. (5) is called the EDPP or the Pna potential, depending on the context. Notice that since $V^{\mathrm{Pa}}(r)$ tends to a finite value at $r=0$, $V^{\mathrm{Pna}}(r,E)$ tends to zero there.

To specify ω in (5) we examine the large-r limit in more detail. The leading energy-independent terms of the polarization potential are[20,43]

$$V^{\mathrm{P(di)}}(r) \underset{\substack{r\to\infty\\E\to 0}}{\sim} -\frac{\alpha}{2r^4}+\frac{3\beta}{r^6}, \tag{6}$$

where

$$\alpha=2\sum_n{}' \frac{|z_{n1}|^2}{\omega_n}, \tag{7}$$

$$\beta=\sum_n{}' \frac{|z_{n1}|^2}{\omega_n^2}, \tag{8}$$

where ω_n is the excitation energy of state n. Making the average-excitation-energy approximation to (6) yields

$$V^{\mathrm{P(di)}}(r) \underset{\substack{r\to\infty\\E\to 0}}{\sim} -\frac{S}{\omega r^4}+\frac{3S}{\omega^2 r^6}. \tag{9}$$

Using calculated values $\alpha=2.359$ (Ref. 7) and $\beta=1.27$ (Ref. 43) for Ne, we eliminate S and obtain $\omega=0.9288$. This is the value we use for ω in the rest of this paper. (For cases where an accurate value of β is unavailable, it is probably sufficient to set ω equal to the ionization potential; for Ne this would have yielded $\omega=0.9705$.[45])

The dispersion relation between the polarization potential and the absorption potential (which is what we call the imaginary part of the optical potential) is[16,17]

$$V^{\mathrm{Pna}}(r,E)=\frac{1}{\pi}\mathscr{P}\int_{\epsilon_{\mathrm{thr}}}^{\infty}\frac{V^{A}(r,\epsilon)}{\epsilon-E}d\epsilon, \tag{10}$$

where $\epsilon_{\rm thr}$ is the lowest excitation energy of the target. In principle, we should solve this equation on the domain $E=(0,\infty)$. For the EDPP, however, we can obtain an analytic solution if we limit the range to $E=(\epsilon_{\rm thr},\infty)$. The analytic solution is[16]

$$V^{A\,\rm disp}(r,E)=\frac{V^{\rm Pna}(r,E)(E-\epsilon_{\rm thr})^{1/2}}{[\epsilon_{\rm thr}+(\omega^2r^2/12)]^{1/2}}\ , \tag{11}$$

where $V^{\rm Pna}(r,E)$ is given by (5). Notice that the only input to both $V^{Pna}(r,E)$ and $V^{A}(r,E)$ is $V^{\rm Pa}(r)$ and ω or, in the present case, $V^{\rm Pa}(r)$ and β. Since both $V^{\rm Pa}(r)$ and β are obtained from *ab initio* calculations,[7,43] the whole optical-model potential is *ab initio*, i.e., nonempirical, except for the steps leading to Eq. (5), which is ultimately justified or not at small r by its success or lack thereof in scattering calculations.

The real part of the complete optical potential is the sum of $V^{\rm Pna}(r,E)$ and the static-exchange potential $V^{\rm SE}(r,E)$. The exchange part of the latter is evaluated by the semiclassical exchange[46] approximation. The static potential and the target charge density needed to calculate the exchange potential are evaluated from the analytic fits of Strand and Bonham.[47]

The calculations by this method are finished by solving the single-channel optical-model-potential Schrödinger equation

$$\left[-\frac{1}{2}\frac{d^2}{dr^2}+\frac{l(l+1)}{2r^2}+V^{\rm SE}(r,E)+V^{\rm P}(r,E)+iV^{A}(r,E)\right]f(r,l,E)=0 \tag{12}$$

for the scattering wave function $f(r,l,E)$ and extracting the complex phase shift $\eta(l,E)$ from

$$f(r,l,E)\underset{r\to\infty}{\sim}(\text{const})\sin[kr-\tfrac{1}{2}l\pi+\eta(l,E)]\ . \tag{13}$$

Alternatively we obtain $\eta(l,E)$ by solving the complex phase equation.[48,49]

B. Matrix effective potential

In the MEP method we replace (12) by a two-channel effective Schrödinger equation,

$$\left[-\frac{1}{2}\frac{d^2}{dr^2}+\frac{l(l+1)}{2r^2}+V^{\rm SE}(r,E)-\frac{k_i^2}{2}\right]f_i(r,l,E)=\sum_{j\neq i}V_{ij}(r,E)f_j(r,l,E) \tag{14}$$

with boundary conditions

$$f_1(r,l,E)\underset{r\to\infty}{\sim}\exp[-i(k_1r-\tfrac{1}{2}l\pi)]-(k_2/k_1)^{1/2}\exp[2i\eta_l(l,E)+i(k_1r-\tfrac{1}{2}l\pi)]\ , \tag{15}$$

$$f_2(r,l,E)\sim(\text{const})\exp(ik_2r)\ . \tag{16}$$

The static-exchange potential $V^{\rm SE}(r,E)$ is the ground-state one of Sec. II A. We require the equations to be Hermitian with $V_{12}(r)$ real and equal to $V_{21}(r)$. Thus the only quantity not defined yet is $V_{12}(r)$. We determine it so that the adiabatic polarization potential implicit in (14) is equal to the variationally computed adiabatic polarization potential $V^{\rm Pa}(r,E)$. This yields

$$\det\begin{bmatrix}-V^{\rm Pa}(r) & V_{12}(r)\\ V_{12}(r) & \omega-V^{\rm Pa}(r)\end{bmatrix}=0\ , \tag{17}$$

where ω is the effective excitation energy

$$\omega=(k_1^2/2)-(k_2^2/2)\ . \tag{18}$$

Solving (17) yields

$$V_{12}(r)=\{[V^{\rm Pa}(r)]^2-\omega V^{\rm Pa}(r)\}^{1/2}\ . \tag{19}$$

Since $V^{\rm Pa}(r)$ is attractive, both terms in the radicand of (19) are positive everywhere; thus $V_{12}(r)$ may be taken as real and positive everywhere. In the perturbation theory limit (19) reduces to the result used previously.[18,21] We take $\omega=0.9288$ as in Sec. A.

C. Phenomenological optical potentials

In this paper we consider two phenomenological approaches to obtaining the absorption part of the

optical potential, namely, the form suggested by Green *et al.*[9] and a form based on the work of Furness and McCarthy[10] and McCarthy *et al.*[11] The real part of the optical potential for both these models was taken as

$$\mathrm{Re}V^{\mathrm{opt}}(r,E)=V^{\mathrm{SE}}(r,E)+V^{\mathrm{Pna}}(r,E)\ , \tag{20}$$

where $V^{\mathrm{SE}}(r,E)$ and $V^{\mathrm{Pna}}(r,E)$ are the static-exchange and nonadiabatic polarization potential of Sec. II A.

The absorption potential of Green *et al.* will be called A_1. Its energy dependence is based on the requirement that it approach the high-energy limit of the inelastic cross section, and its r dependence is based on an analogy to the static potential. The energy-dependent factor contains parameters adjusted to the experimental[40] absorption cross section. Further details and the values of parameters are given in Refs. 9 and 22.

The second phenomenological model considered here for the absorption potential will be called A_2. It is based on the suggestions of McCarthy *et al.*[11] This model assumes that the absorption potential at a given point is proportional to the radial density of the highest-energy valence orbital and the energy-dependent Rutherford cross section at the point, where the relevant energy is the local kinetic energy estimated on the basis of the real part of the optical potential at the given point. We take the real part of the optical potential to be the same as in Sec. II A. The proportionality constant is adjusted to yield agreement with the experimental[40] absorption cross sections. The resulting absorption potential is

$$V^{A_2}(r,E)=-\frac{W^{A_2}(E)\,|\,r\phi_{2p,\mathrm{Ne}}(r)\,|^2}{[E-V^{\mathrm{SEPna}}(r,E)]^2} \tag{21}$$

where[50]

$$r\phi_{2p,\mathrm{Ne}}=Nr(0.715\,07r\,e^{-2.0514r}+0.370\,89r\,e^{-4.674\,77r}) \tag{22}$$

and N is the radial normalization constant ($N=9.759\,624$). We further write $W^{A_2}(E)$ as

$$W^{A_2}(E)=C(E)(E-\epsilon_{\mathrm{thr}}) \tag{23}$$

and we adjust the parameter $C(E)$ at each energy.

Equations (21)–(23) are based on and are very similar to those used by McCarthy *et al.*,[11] but those workers did not give enough information for us to reproduce their potential. Furthermore their published absorption cross sections do not agree with experiment. Thus we independently adjusted the parameter $C(E)$, and hence $W^{A_2}(E)$, for the above specified functional form in order to compare their method to the new methods studied here.

III. CALCULATIONS, POTENTIALS, AND RESULTS

The numerical methods used for the calculations are the same as used in our previous work.[16,22] The adjusted values of $W^{A_2}(E)$ for three impact energies are given in Table I, and the three different absorption potentials for these energies are shown in Figs. 1–3. These figures also show $V^{A_1}(r,E)$ and $V^{A_2}(r,E)$ at these energies.

Some values of the calculated phase shifts are given in Tables II–IV where they are compared to experimental values[39] at 10 eV, previous theoretical values[26–28,31] at 8.7–54.4 eV, and each other at 30–100 eV. The calculated integral cross sections σ_{el} and momentum-transfer cross sections σ_{el}^{m} for elastic scattering and the absorption and total cross sections σ_{abs} and σ_{tot}, are given in Tables V–VII, where they are compared to experiment.[33–35,37–42] Table VII also includes some comparisons to previous theoretical calculations.[11,29,30] The differential elastic cross sections are given in Table VIII and Figures 4–7; comparisons to experimental[34–37,39] and previous theoretical[11,28] work are given in both

TABLE I. Empirical values of the proportionality constant and pre-radial-density factor in the absorption potential A_2.

E	W^{A_2}		$\frac{W^{A_2}}{[E-V^{\mathrm{SEPna}}(r)]^2}$ (a.u.)		
(ev)	(a.u)	$r=0.5a_0$	$1.0a_0$	$2.0a_0$	$3.0a_0$
30	4.10	6.39(−2)	6.52(−1)	2.94	3.32
50	29.5	3.93(−1)	3.04	8.21	8.69
100	241.5	2.25	10.5	17.5	17.8

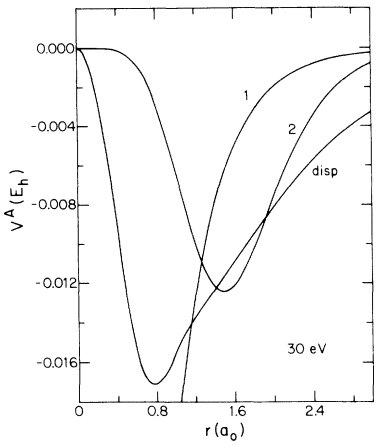

FIG. 1. Absorption potentials for 30-eV impact energy as functions of the distance of the scattering electron from the nucleus. Curve corresponding to the phenomenological potential A_1 of Green *et al.* is labeled "1," the phenomenological potential A_2 is labeled "2," and the potential obtained from the dispersion relation is labeled "disp."

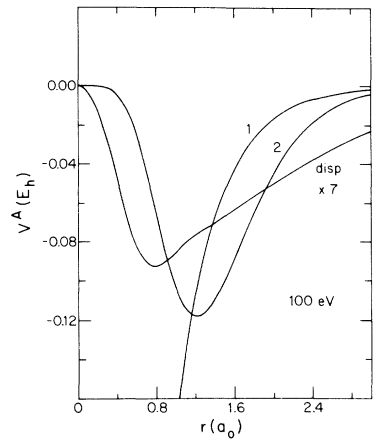

FIG. 3. Same as Fig. 1 except for 100 eV and the absorption potential obtained from the dispersion relation has been magnified seven times for this plot.

places. (The experimental differential cross sections in Fig. 4 were regenerated by the prescription of Williams,[39] i.e., we use his tabulated phase shifts for s, p, and d waves and polarized Born phase shifts for $l=3-20$. The theoretical results at this energy are based on numerical phase shifts for $l=0-7$ and polarized Born phase shifts for $l=8-20$. At higher energies the theoretical results are based on increasingly more partial waves, as required for convergence.)

Before beginning the discussion, we summarize our notation. Capital letters are used for the four types of potentials: static (S), exchange (E), polarization (P), and absorption (A). The S and E parts are always the same. Polarization, when included, is either adiabatic (Pa) or nonadiabatic (Pna, i.e., EDPP). Absorption, when included, is given by the model of Green *et al.* (A_1), by our adjustment of the form used by McCarthy *et al.* (A_2), or by the nonadjusted potential calculated from the Pna potential and the dispersion relation (A_{disp}). The matrix effective potential includes polarization and absorption implicitly rather than through P or A terms, and it is denoted MEP.

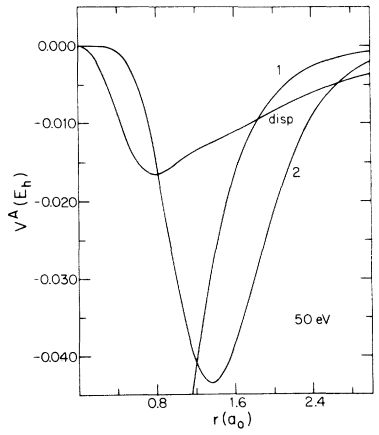

FIG. 2. Same as Fig. 1 except for 50 eV.

IV. DISUCSSION AND COMPARISON TO EXPERIMENT

A. Above threshold

1. Phase shifts

Tables III and IV compare phase shifts for small-l and for some typical larger-l values. The tables show that the real parts of the phase shifts are not strongly affected by the absorption potential but depend mainly on the real part of the polarization potential. As expected $\mathrm{Re}\eta_l$ is largest for the adiabatic polarization potential and smallest for the static-exchange case in which the real polarization potential is neglected. In fact, these two models, SEPa and SE, provide physical limits for the maximum and minimum contributions of charge polarization. For $E \leq 30$ eV and small l, the SEPna results are midway between these limits, but at higher energies the SEPna results for small l are very simi-

TABLE II. Comparison of phase shifts at 10 eV for s, p, d waves for various theoretical models and experiment.

	Phase shift (rad, mod π)				
l	SEPa	SEPna	SE	MEP	Expt.[a]
0	2.528	2.307	2.242	0.470	2.342
1	3.112	2.870	2.814	0.096	2.922
2	0.106	0.081	0.046	0.137	0.076

[a]Williams, Ref. 39.

lar to the SE ones. At large l the SEPna and SEPa results are very similar to each other but differ from the SE results. This is a consequence of the fact that the large-l scattering depends mainly on the large-r tail of the potential where the SEPa and SEPna potentials both tend to $-\alpha/(2r^4)$ but where the SE potential is much smaller.

The real part of η_l as computed by the MEP method is large; in fact, it sometimes even exceeds the SEPa value. This is somewhat surprising in light of the fact, already mentioned, that we would expect the SEPa model to yield the maximum possible amount of polarization. Yet the MEP model, which takes polarization into account in a dynamic way, leads to an even more attractive effect on the phase shift. A similar effect was found in previous work on He (Ref. 18) and on high-energy scattering by Ne,[22] and we also note that the eikonal optical model leads to a polarization effect that exceeds the adiabatic one.[29] This calculated effect is surprising, and it requires further study before we can accept it as a true description of the physical dynamics.

Next consider the imaginary parts of the phase shifts. These are always less than the real parts. The imaginary parts calculated using A_{disp} decrease least rapidly with l, and for large l, $\text{Im}\eta_l$ calculated by this method exceeds the values calculated by other methods by an order of magnitude or more. This result is consistent with Figs. 1–3, which show that A_{disp} is longer in range than A_1 and A_2. The MEP method yields the largest imaginary parts of the phase shifts for $l=0$, but $\text{Im}\eta_l$ calculated by this method decreases very rapidly with increasing l.

Finally we note that the choice of real polarization potential has more effect on $\text{Im}\eta_l$ than the choice of absorption potential has on $\text{Re}\eta_l$. Compare, for example, the $l=0-2$ phase shifts calculated by the SEPaA_1 and SEPnaA_1 methods. This effect is larger at 30 eV than at the higher energies.

2. Differential cross sections

Next consider Figs. 5–7 and Table VIII. Figure 5 shows that the MEP differential cross section has a qualitatively incorrect shape at 30 eV. In contrast the SEPnaA_{disp} model leads to excellent agreement with experiment at this energy for $\theta > 40°$. For $\theta \leq 40°$ this model overestimates the cross section, with the error increasing to 37% at 20°. The SEPnaA_2 and SEPnaA_1 models predict results similar to the SEPnaA_{disp} model at 30 eV. The overall good agreement of the SEPnaA_{disp} calculations with experiment at this energy is very encouraging because, unlike the SEPnaA_1 and SEPnaA_2 models, the SEPnaA_{disp} model has no adjustable parameters. We note that the SEPnaA_{disp} model is also very successful for e-He scattering at low energies.[16] In contrast, however, we note that the SEPnaA_1 model underestimated the differential cross sections at both small and large θ for e-Ne scattering at 150–700 eV.[22]

Figure 6 shows that the MEP model is becoming more accurate as the energy is raised. However, the MEP differential cross section is significantly too large for $\theta < 30°$ and significantly too small for $\theta > 105°$. Again at 50 eV the SEPnaA_1, SEPnaA_2, and SEPnaA_{disp} results are in good agreement with each other and with experiment. Although the two sets of experimental results are in generally good agreement with each other, they do differ by a factor of 1.12 at 120°, 1.37 at 60°, and even more near the minimum. If we consider the experimental uncertainty to be 37% in general, and larger near the minimum, then all three SEPna$A$ models agree with the experimental results within experimental error. The agreement of the SEPnaA_{disp} results with the experiments is the best. The SEPaA_1 potential predicts more forward scattering than the SEPnaA_1 and SEPnaA_{disp} potentials. The SEPaA_1 results do not agree as well with experiment as the SEPna$A$ results do, but the difference appears to be only

TABLE III. Comparison of phase shifts (rad, modπ) calculated by various methods to previous theoretical values.

E (eV)	$k(a_0^{-1})$	l	SEPa	SEPna	SEPaA_1	SEPnaA_1	SEPnaA_{disp}	MEP	Expt.[a]	Thompson[b]	Garbaty-LaBahn[c]	Yau *et al.*[d]	Fon-Berrington[e]
8.71	0.8	0	2.595	2.380				1.619	2.397	2.407	2.397	2.393	2.398
		1	3.135	2.910				0.041	2.955	2.969	2.963	2.950	2.956
		2	0.089	0.072				0.084	0.063	0.075	0.071	0.075	
		3	0.018	0.015				0.017				0.019	
		4	0.007	0.006				0.007					
13.61	1.0	0	2.361	2.133				0.406	2.213	2.196	2.185	2.184	2.181
		1	3.048	2.772				3.126	2.846	2.857	2.851	2.846	2.852
		2	0.154	0.110				0.146	0.120	0.132	0.125	0.129	
		3	0.031	0.022				0.029		0.029		0.032	
		4	0.012	0.009				0.011		0.012			
34.83	1.6	0	1.768	1.530	$1.768+i0.027$	$1.530+i0.029$	$1.530+i0.016$	$1.138+i0.116$		1.702			
		1	2.750	2.435	$2.750+i0.035$	$2.436+i0.043$	$2.435+i0.017$	$2.973+i0.350$		2.540			
		2	0.415	0.265	$0.414+i0.015$	$0.265+i0.012$	$0.265+i0.020$	$0.425+i0.011$		0.453			
		3	0.092	0.052	$0.092+i0.002$	$0.052+i0.002$	$0.052+i0.011$	$0.094+i0.002$		0.108			
		4	0.034	0.017	$0.034+i0.001$	$0.017+i0.001$	$0.017+i0.007$	$0.034+i0.0004$		0.042			
54.42	2.0	0	1.450	1.220	$1.450+i0.070$	$1.221+i0.070$	$1.220+i0.013$	$1.427+i0.161$		1.326			
		1	2.574	2.274	$2.578+i0.086$	$2.277+i0.099$	$2.274+i0.014$	$2.615+i0.252$		2.372			
		2	0.587	0.387	$0.585+i0.052$	$0.385+i0.042$	$0.387+i0.018$	$0.615+i0.061$		0.527			
		3	0.147	0.084	$0.147+i0.011$	$0.084+i0.010$	$0.084+i0.012$	$0.155+i0.018$		0.134			
		4	0.056	0.026	$0.056+i0.004$	$0.011+i0.001$	$0.026+i0.009$	$0.056+i0.007$		0.053			

[a]Williams, Ref. 39.
[b]Reference 26.
[c]Reference 27.
[d]Reference 31.
[e]Reference 32.

TABLE IV. Comparison of phase shifts (rad, mod π) for selected l values for various potentials.

E (eV)	l	SEPa	SEPna	SE	SEPaA_1	SEPnaA_1	SEA_1	SEPnaA_2	SEPnaA_{disp}	MEP
30	0	1.87	1.64	1.61	1.87 +i0.018	1.63 +i0.019	1.61 +i0.019	1.63 +i0.009	1.63 +i0.016	1.25 +i0.087
	1	2.81	2.49	2.47	2.81 +i0.023	2.49 +i0.028	2.47 +i0.028	2.49 +i0.008	2.49 +i0.017	0.072+i0.119
	2	0.362	0.232	0.205	0.362+i0.008	0.232+i0.006	0.246+i0.006	0.232+i0.013	2.32 +i0.019	0.394+i0.003
	6	0.008	0.005	2(−4)	0.008+i2(−5)	0.005+i2(−5)	2(−4)+i2(−5)	0.005+i4(−5)	0.005+i0.002	0.013+i4(−7)
	10	0.002	0.002	2(−6)	0.002+i2(−7)	0.002+i2(−7)	2(−6)+i2(−7)	0.002+i3(−8)	0.002+i4(−4)	0.003+i1(−8)
50	0	1.51	1.28	1.27	1.51 +i0.058	1.28 +i0.061	1.27 +i0.061	1.28 +i0.026	1.28 +i0.014	1.51 +i0.156
	1	2.61	2.30	2.29	2.61 +i0.075	2.31 +i0.087	2.29 +i0.087	2.30 +i0.026	2.30 +i0.015	2.67 +i0.254
	2	0.553	0.362	0.345	0.552+i0.043	0.361+i0.034	0.344+i0.034	0.361+i0.045	0.362+i0.019	0.598+i0.049
	6	0.014	0.006	9(−4)	0.014+i3(−4)	0.006+i3(−4)	9(−4)+i3(−4)	0.006+i7(−4)	0.006+i0.004	0.020+i7(−4)
	10	0.003	0.002	1(−5)	0.003+i6(−6)	0.002+i6(−6)	1(−5)+i6(−6)	0.002+i3(−6)	0.002+i0.001	0.005+i2(−6)
100	0	0.996	0.790	0.784	0.997+i0.136	0.792+i0.143	0.786+i0.142	0.790+i0.049	0.790+i0.009	0.932+i0.162
	1	2.32	2.07	2.06	2.33 +i0.175	2.07 +i0.190	2.07 +i0.190	2.07 +i0.053	2.07 +i0.010	0.859+i0.231
	2	0.807	0.575	0.568	0.803+i0.136	0.570+i0.122	0.564+i0.122	0.576+i0.078	0.575+i0.012	0.810+i0.151
	6	0.029	0.009	0.006	0.029+i0.004	0.009+i0.004	0.006+i4(−4)	0.009+i0.009	0.009+i0.005	0.034+i0.009
	10	0.006	0.002	9(−5)	0.006+i2(−4)	0.002+i2(−4)	9(−5)+i2(−4)	0.002+i2(−4)	0.002+i0.002	0.009+i0.002

TABLE V. Integral and momentum transfer cross sections (a_0^2) at 10 eV (at this energy, $\sigma_{\text{el}}=\sigma_{\text{tot}}$).

	σ_{el}	σ_{el}^m
Experimental results		
Salop and Nakano[a]	11.9	
Stein *et al.*[b]	12.2	
Williams[c]	11.8	8.23
Previous theoretical results		
Fon and Berrington[d]	12.5	7.92
Present theoretical results		
SEPa	6.77	6.23
SEPna	13.7	9.17
SE	16.0	9.67
MEP	15.9	15.5

[a]Reference 33.
[b]Reference 38.
[c]Reference 39.
[d]Reference 32.

slightly larger than the experimental uncertainty.

At 100 eV there again appears to be considerable uncertainty in the experimental values. At this energy the accuracy of the MEP calculation for $\theta \leq 40°$ is much improved. Beyond 40° though the MEP results appear to be too small except near the minimum. The SEPnaA_{disp} model again appears to be the overall most accurate one at this energy although it may be beginning to underestimate the forward peak.

3. *Integral cross sections*

Now consider Tables VI and VII. At 30 eV the average experimental value of the elastic integral cross section is 11.8 a_0^2. The SEPna and the various SEPna$A$ models overestimate this by 10−13%, the SEPa and SEPaA_1 models underestimate it by 8−10%, and the MEP model underestimates it by 21%. The absorption cross section proves to be harder to calculate. Both totally *ab initio* models (SEPnaA_{disp} and MEP) overestimate it by a factor of 2.8 or more.

At 50 eV the average experimental value for the elastic cross section is 11.2a_0^2. The MEP model underestimates this by only 11%, but it still overesti-

TABLE VI. Integral and momentum-transfer cross section at impact energies 30—100 eV.

E (eV)	SEPnaA_{disp} σ_{el}	SEPnaA_{disp} σ_{abs}	SEPnaA_{disp} σ_{tot}	Experiment[a] σ_{el}	Experiment[a] σ_{abs}	Experiment[a] σ_{tot}
30	13.2	2.48	15.6	11.3	0.754	12.1
40	11.9	2.36	14.2	10.7	1.35	12.1
50	9.76	1.81	11.6	10.8	1.85	12.7
60	9.90	2.05	11.9	10.4	2.24	12.6
70	9.17	1.90	11.1	9.99	2.53	12.5
80	8.55	1.78	10.3	9.57	2.71	12.3
90	8.03	1.66	9.69	9.15	2.85	12.0
100	7.57	1.56	9.13	8.74	2.92	11.7

[a]Wagenaar and deHeer, Ref. 41.

mates the absorption cross section by a factor of 1.8. In contrast the SEPnaA_{disp} predicts σ_{el} within 4% and σ_{abs} within 19%.

At 100 eV the average experimental elastic cross section is $8.82a_0^2$. The MEP and SEPnaA_{disp} models underestimate this by 17% and 14%, respectively, and they incorrectly estimate σ_{abs} by larger factors, a factor of 1.32 for MEP and 0.53 for SEPnaA_{disp}. The trend is clear that the accuracy of the MEP is increasing as the energy is increased, and the SEPnaA_{disp} potential is shifting from overestimating the cross sections at energies a little above the inelastic threshold to underestimating them at the upper end of the intermediate energy regime. The latter trend is very clear in Table VI.

Table VII shows that ignoring the absorption potential does not affect the elastic cross sections very significantly at these energies; compare, for example, the SEPna results to the SEPnaA_2 or SEPnaA_{disp} results. This is very interesting because we found previously[22] that the neglect of absorption has considerable effect of σ_{el} for e-Ne scattering at higher energies.

4. *Absorption potentials*

Now consider Fig. 1—3 and Table I. The first interesting feature is the different shapes, as functions of r, of $V^{A_1}(r,E)$ and $V^{A_2}(r,E)$. As a consequence of the different shapes, when the two potentials are adjusted to both yield the experimental absorption cross sections, they have different energy dependences. Potential A_1 factors into an E-dependent coefficient and an r-dependent shape factor, which is strong at small r. Potential A_2 is nonseparable with peaks in the range $1.2-1.6a_0$. Both Table I and Fig. 1—3 show that $V^{A_2}(r,E)$ is relatively longer ranged at lower energies.

An important point to be emphasized here is that one can take an arbitrary functional form for the absorption potential and adjust the parameters to yield experimental absorption cross sections. With such a procedure the strength and shape of the potential will depend on the constraints on its functional form. Nevertheless, Figs. 1—3 show that the A_1 and A_2 absorption potentials are very similar only in the $1-1.5\ a_0$ range.

In contrast to the A_1 and A_2 potentials, whose form is fixed, the shape of the A_{disp} potential is determined by solving the dispersion relation. It is an indirect consequence of the shape and energy dependence of the real Pna potential rather than a consequence of directly modeling the imaginary potential. The present results seem to indicate, however, that the A_{disp} potential has an incorrect energy dependence and is too long ranged. We attribute this to deficiencies in the Pna potential. It would be valuable to develop new models for energy-dependent real polarization potentials and use these with the dispersion relation to attempt to predict more accurate absorption potentials.

B. Below threshold

Tables II and III compare the phase shifts calculated by the SEPa, SEPna, SE, and MEP models for $E < \epsilon_{thr}$ where these phase shifts are real. Table II also compares these phase shifts to the experimental values of Williams. As expected[51] the SEPa phase shifts are too large, which is consistent with the adiabatic polarization potential being too attractive. (The SEPa method in the present notation is called

TABLE VII. Integral elastic, momentum-transfer, absorption, and total cross sections (a_0^2) at impact energies 30–100 eV.

E (eV)	30				50				100			
	σ_{el}	σ_{el}^m	σ_{abs}	σ_{tot}	σ_{el}	σ_{el}^m	σ_{abs}	σ_{tot}	σ_{el}	σ_{el}^m	σ_{abs}	σ_{tot}
Experiment												
Gupta and Rees[a]									8.82[k]	4.54[k]		
Williams and Crowe[b]	12.3				11.8				9.82			
Dubois and Rudd[c]					11.0	9.47[k]			7.90	5.68[k]		
deHeeer *et al.*[d]	11.3		0.754	12.1	10.8		1.85	12.7	8.74		2.92	11.7
Wagenaar and deHeer[e]				13.7				13.1				10.8
Kauppila *et al.*[f]				13.3				12.7				
Theory												
McCarthy *et al.*[g]	13.6[k]	10.7[k]	0.393	14.0	11.2[k]	8.62[k]	1.48	12.7	7.49[k]	4.59[k]	2.78	10.3
Byron and Joachain[h]									6.44[k]	2.07[k]	7.76	14.2
Jhanwar *et al.*[i]									13.0		0.0	13.0
Fon and Berrington[j]	12.7	11.0			11.0	9.23			8.03	5.53		
SE	13.6	10.6	0.0	13.6	11.0	9.24	0.0	11.0	7.65	5.88	0.0	7.65
SEPa	10.9	9.80	0.0	10.9	11.3	9.87	0.0	11.3	9.43	6.61	0.0	9.43
SEPna	13.6	10.7	0.0	13.6	11.1	9.29	0.0	11.1	7.73	5.58	0.0	7.73
SePaA_1	10.6	9.21	0.767	11.0	10.3	7.94	1.86	12.1	7.44	3.86	2.84	10.3
SePnaA_1	13.0	9.94	0.798	13.8	9.76	7.31	1.81	11.6	5.92	3.34	2.76	8.67
SEA_1	13.0	9.82	0.793	13.8	9.63	7.27	1.80	11.4	5.85	3.33	2.75	8.60
SEPnaA_2	13.3	10.3	0.755	14.1	10.5	8.18	1.85	12.4	6.98	4.60	2.91	9.89
SEPnaA_{disp}	13.2	9.98	2.48	15.6	10.8	8.71	2.21	13.0	7.57	5.64	1.56	9.13
MEP	9.27	6.13	2.13	11.4	9.93	6.11	3.40	13.3	7.34	3.46	3.85	11.2

[a]Ref. 34.
[b]Ref. 35.
[c]Ref. 37.
[d]Ref. 40.
[e]Ref. 41.
[f]Ref. 42.
[g]Ref. 11.
[h]Ref. 29.
[i]Ref. 30.
[j]Ref. 32.
[k]These values are not reported by the original authors but are obtained by integration of differential cross sections as in Ref. 22.

TABLE VIII. Differential cross sections at 50 eV.

	$d\sigma_{el}/d\Omega(a_0^2/sr)$								
	Theory					Experiment			
θ (deg)	SEPaA_1	SEPnaA_1	SEPnaA_2	SEPnaA_{disp}	MEP	McCarthy *et al.*[a]	Williams and Crowe[b]	Dubois and Rudd[c]	Fon and Berrington[d]
10	5.04	3.46	3.73	3.75	7.05	4.50		4.33	4.26
15	4.07	3.10	3.35	3.21	5.43	3.78		3.38	
20	3.25	2.76	2.97	2.78	4.14	3.17	2.67	2.75	2.86
30	2.00	2.10	2.23	2.07	2.33	2.26	2.13	1.96	1.99
60	0.736	0.836	0.852	0.913	0.596	0.904	1.06	0.812	0.882
90	0.206	0.128	0.127	0.150	0.197	0.138	0.156	0.211	0.199
120	0.152	0.197	0.250	0.253	0.0739	0.246	0.229	0.260	0.201
150	1.44	1.93	1.42	1.53	1.10	1.49	1.87	1.74	1.65

[a]Reference 11.
[b]Reference 35.
[c]Reference 37.
[d]Reference 32.

AET by Callaway, and our findings here are similar to his conclusions for e-H triplet scattering.) The SEPna phase shifts are much more accurate and differ from the experimental values by less than 2% for s and p waves and by 7% for d waves at 10 eV. (We should not neglect to mention the possibility of experimental error. The $l=2$ phase shift is particularly sensitive to the type of analysis used by Williams, and it is not clear whether we can exclude a phase shift as large as 0.09 on the basis of his results. This could change our conclusions to a small degree.) Assuming no significant experimental error we see that the low-energy SEPna phase shifts are remarkably accurate for Ne, and we recall that this was the case for He too.[18] As a consequence of the accurate phase shifts the low-energy differential cross section predicted by the SEPna method is in excellent agreement with experiment; see Fig. 4. The integral and momentum-transfer cross sections predicted by this model are about 10–15 % high at

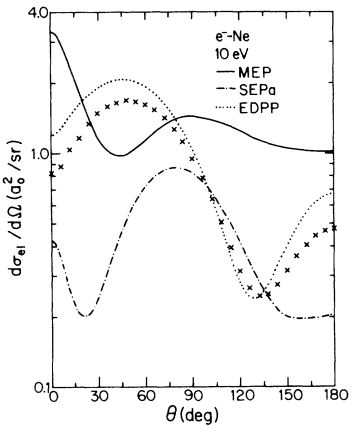

FIG. 4. Differential cross section for 10-eV impact energy as functions of scattering angle. Theoretical curves are shown as solid (MEP), dash-dot-dash (SEPa), and dotted (SEPna) curves. Experimental results of Williams are shown as ×'s.

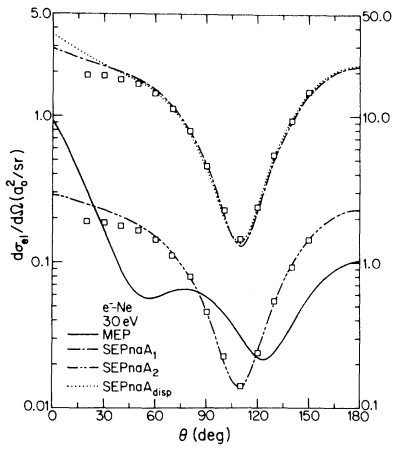

FIG. 5. Differential cross sections for 30-eV impact energy as functions of scattering angle. SEPnaA_1 (long-short-long dashes) and SEPnaA_{disp} (dotted) curves and the experimental results of Williams and Crowe are shown in the top part of the figure for which the scale is given on the left. MEP (solid) and SEPnaA_2 (long-short-short-long dashes) curves are shown in the bottom half of the figure for which the scale is shown on the right. Experimental results are also repeated in the bottom for comparison.

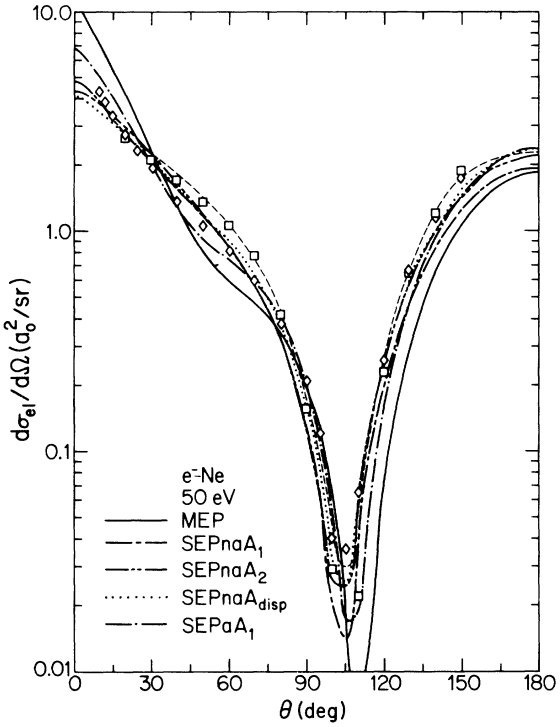

FIG. 6. Differential cross sections for 50-eV impact energy as functions of scattering angle. Present theoretical results are shown as a thick solid curve (MEP), long-short dashed curve (SEPnaA_1), long-short-short dashed curve (SEPnaA_2), dotted curve (SePnaA_{disp}), and dash-dot curve (SEPaA_1). Theoretical results of Blum and Burke for 27°—180° are shown as a thin dashed curve, they did not publish results for $\theta < 27°$ at this energy. Experimental results of Williams and Crowe are shown as squares and those of Dubois and Rudd are shown as diamonds.

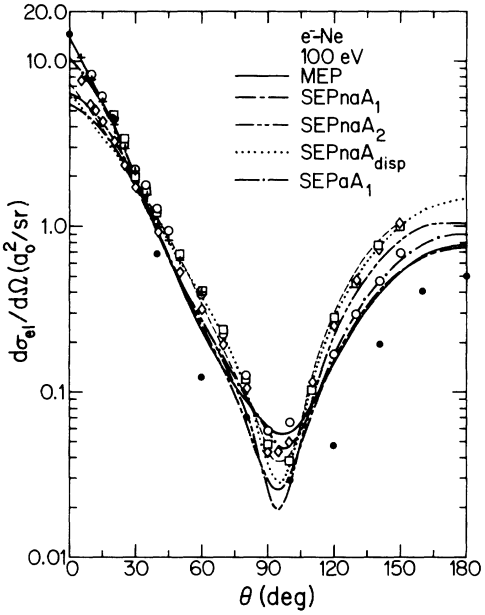

FIG. 7. Same as Fig. 6 except for 100-eV, SEPaA_1 is not shown, the Blum-Burke results are available for 0°—150° at this energy, the Byron-Joachain eikonal-optical-model calculations are shown as filled-in circles, and two additional sets of experimental results are shown: those of Gupta and Rees as circles and those of Jansen *et al.* as +'s.

10 eV; see Table V. Tables II and V and Fig. 4 indicate that the MEP model is not very accurate at 10 eV for Ne.

The error in the SEPa cross sections at 10 eV is exaggerated by the fact that the SEPa p-wave phase shift is accidentally very close to π at 10 eV. When examined in detail this explains why the SEPa cross sections are actually smaller than the experimental ones at this energy.

V. COMPARISON TO PREVIOUS THEORETICAL WORK

The present results are compared to the results of some previous theoretical calculations[11,26—32] in Tables III, VII, and VIII and in Figs. 6 and 7. Some of the real polarization potentials used by previous workers are compared to those used here for an impact energy of 100 eV in Table IX. We will discuss these comparisons in chronological order of the previous approaches.

Thompson[26] used an SEP-type model with an adiabatic polarization potential based on the polarized orbital method. A theoretical problem with the polarization potential he used is that it includes only dipole contributions whereas our results include all multipoles. For low l Thompson's phase shifts are intermediate between the SEPa and SEPna phase shifts of the present work. They are closer to the SEPna phase shifts at low energy where the SEPna phase shifts are very accurate, and they are closer to midway between the SEPa and SEPna phase shifts at 35—54 eV. At higher l Thompson's phase shifts do not decrease as rapidly as the SEPa and SEPna phase shifts.

Garbaty and LaBahn[27] performed full polarized orbital calculations, still including only dipole effects. The full polarized orbital method takes some account of nonadiabatic effects; their results are very close to Thompson's.

Blum and Burke[28] and Fon and Berrington[32] performed pseudostate close-coupling calculations. From the perspective of the present paper this method may be considered to be a variational (in a

TABLE IX. Real polarization potentials (in E_h) for an impact energy of 100 eV.

$r(a_0)$	$V^{Pa}(r)$[a]	$V^{Pa}(r)$[b]	EDPP[c]	Byron and Joachain[d]	Jhanwar *et al.*[e]
0.01	−1.0	−3.0(−3)	−2.0(−6)	−7.0(1)	−3.1(−3)
0.25	−1.1	−5.3(−2)	−1.3(−3)	−2.2	−2.2
0.50	−9.0(−1)	−7.3(−2)	−4.4(−3)	−8.9(−1)	−4.1
0.75	−5.6(−1)	−7.6(−2)	−6.1(−3)	−4.7(−1)	−2.6
1.00	−3.0(−1)	−7.0(−2)	−5.8(−3)	−2.8(−1)	−1.3
1.25	−1.8(−1)	−6.0(−2)	−5.3(−3)	−1.8(−1)	−6.0(−1)
1.50	−1.2(−1)	−5.0(−2)	−4.9(−3)	−1.2(−1)	−3.1(−1)
2.00	−5.4(−2)	−3.2(−2)	−3.9(−3)	−5.9(−2)	−9.8(−2)
2.50	−2.7(−2)	−2.0(−2)	−2.9(−3)	−3.1(−2)	−3.9(−2)
3.00	−1.4(−2)	−1.2(−2)	−2.1(−3)	−1.8(−2)	−1.8(−2)
3.50	−8.0(−3)	−7.6(−3)	−1.5(−3)	−1.0(−2)	−9.7(−3)
4.00	−4.8(−3)	−4.8(−3)	−1.1(−3)	−6.3(−3)	−5.6(−3)
5.00	−1.9(−3)	−2.1(−3)	−6.4(−4)	−2.6(−3)	−2.3(−3)
6.00	−9.3(−4)	−1.0(−3)	−3.8(−4)	−1.2(−3)	−1.1(−3)
8.00	−2.9(−4)	−3.3(−4)	−1.6(−4)	−3.6(−4)	−3.3(−4)
10.00	−1.2(−4)	−1.3(−4)	−7.9(−5)	−1.4(−4)	−1.4(−4)

[a]Reference 7.
[b]Reference 11 with $\alpha = 2.687 a_0^3$.
[c]Equation (5) and V^{Pa} of Ref. 7.
[d]Reference 29.
[e]Reference 30.

scattering sense rather than a polarization-potential sense) analog of the MEP method. However, their pseudo states include only S→P polarization effects and lead to an arbitrary effective polarization potential at small r, while the MEP method includes contributions from all symmetries and yields the full response in the adiabatic approximation at all r. The figures imply that the Blum-Burke cross sections are more accurate than the MEP ones at large scattering angles for 50 and 100 eV and small scattering angles at 50 eV. At 100 eV the MEP results give more accurate small-angle scattering. As discussed by Walters,[52] the underestimate of small-angle, high-energy scattering by the pseudostate method may be a consequence of the implicit polarization potential in this method. It is encouraging that the MEP method, with its more complete account of polarization effects, does not appear to suffer from this systematic error. The calculations of Fon and Berrington[32] (not shown in the figures, but see Table VIII) appear to be more accurate than those of Blum and Burke at small angles, and this complicates the above discussion. Blum and Burke did not tabulate phase shifts but their plot shows that their low-energy phase shifts are somewhat smaller than Thompson's. The available phase shifts from the calculations for Fon and Berrington are compared to the other calculations in Table III. Overall the Fon-Berrington calculations appear to be the most accurate available calculations over the whole energy range considered here.

Byron and Joachain[29] studied e-Ne scattering with the eikonal-optical-model formalism at energies of 100 eV and higher; we can compare with their results at 100 eV. Table VII shows that their absorption potential is much too high, and their elastic integral and momentum-transfer cross sections are too low. The MEP model is much more accurate for these three quantities. Figure 7 shows that the eikonal optical model is less successful than any of the present calculations for the medium- and large-angle elastic differential cross section. Table IX shows that for $r \geq 0.5a_0$, the real polarization potential used by Byron and Joachain is either very similar to or a little more attractive than the adiabatic polarization potential of Ref. 7.

The phenomenological-optical-model calculations of McCarthy *et al.*[11] are the original versions of the SEPaA_2 calculations of the present study. However, as discussed above and as illustrated in Table VII, McCarthy *et al.* did not adjust σ_{abs} to experiment as closely as is done here. Their results need not be discussed further since our SEPaA_2 calculations are discussed extensively above. The comparison of Table IX does merit a comment though. Although McCarthy *et al.*'s polarization potential is in principle adiabatic, they use a Temkin-Lamkin approximation and a hydrogenic approximation.

The Temkin-Lamkin approximation neglects all multipoles except the dipole and it includes only contributions to the integrals from the region where the scattering electron is further from the nucleus than a bound electron. Because of the Temkin-Lamkin approximation, $V^{\mathrm{Pa}}(r)$ of Ref. 11 is much less attractive than that of Ref. 7 for $r < 3a_0$.

Jhanwar *et al.*[30] applied an SEP-type model (in addition to less complete models not considered here) at energies 100 eV and higher. Their polarization potential is energy dependent, like the present Pna potential, and thus it is especially interesting to compare their results to ours. Table VII shows that their calculations seriously overestimate the elastic integral cross section. Their 100-eV differential cross section, not shown here, has a minimum value of 0.24 a_0^2/sr and a 180° local maximum of $2.7a_0^2$/sr. Reference to Fig. 7 shows that both of these values are too high. One reason for the overestimate may be their polarization potential. Table IX shows that this is much too attractive at small r.

Yau *et al.*[31] performed another polarized-orbital—type SEP calculation, with special emphasis on the exchange potential and with inclusion of all multipoles in the polarization potential. Their results are very close to Thompson's and Garbaty and LaBahn's.

VI. CONCLUSIONS

We have tested three approaches to the treatment of electronic polarization and absorption effects in electron scattering by applying them to e-Ne scattering in the difficult intermediate-energy range of 10—100 eV. The nonadiabatic energy-dependent-polarization-potential method is most successful at low energy but it leads by the dispersion relation to a nonempirical absorption potential that appears too long ranged and that decreases too rapidly at high energy. The matrix-effective-potential method appears to be most accurate at high energy for Ne; at low energy it overestimates the absorption cross section and predicts an incorrect angular dependence for the differential cross sections. The use of phenomenological absorption potentials is capable of yielding high-accuracy elastic differential cross sections even with considerably different shapes for the r dependence of the absorption potential. We think these tests provide useful calibration points so that we can better estimate how much to trust these kinds of methods for problems where the experimental data are less complete.

VII. MICROFICHE SUPPLEMENT

We are submitting six tables of additional data to Physics Auxiliary Publication Service.[54] This includes differential elastic cross sections calculated by the MEP, SEPnaA_1, SEPnaA_2, and SEPnaA_{disp} methods at 10, 30, 50, and 100 eV and partial-wave elastic and absorption cross sections calculated by these methods at 30, 50, and 100 eV.

Note added in proof. We can now compare to the new experimental results of Brewer *et al.*[53] at 10 eV. Their phase shifts and cross sections are 2.336(s), 2.908(p), 0.087(d), $12.4\,a_0^2(\sigma_{\mathrm{el}})$, and $8.7\,a_0^2(\sigma_{\mathrm{el}}^m)$; these values compare well to the present SEPna results in Tables II and V. Brewer *et al.* measured $d\sigma_{\mathrm{el}}/d\Omega$ for $\theta = 20-120°$. Their results agree with the values we calculated from Williams' phase shifts within 7% or better at all angles in this range, but are systematically closer to the present SEPna calculations than Williams' results are. The SEPna differential cross section agrees with that of Brewer *et al.* within 10% for 65—120°, but the difference increases to a factor of 1.33 at 20°.

ACKNOWLEDGMENTS

This work was supported in part by the National Science Foundation under Grant No. CHE80-25232. We are grateful to Dr. A.E.S. Green for an advance copy of Ref. 9.

[1]See, e.g., R. K. Nesbet, Adv. Quantum Chem. 9, 215 (1975); Adv. At. Mol. Phys. 13, 315 (1977); W. P. Reinhardt, Nucl. Phys. A353, 295c (1981).

[2]N. F. Lane and R. J. W. Henry, Phys. Rev. 173, 183 (1968).

[3]S. Hara, J. Phys. Soc. Jpn. 27, 1262 (1969).

[4]D. G. Truhlar, D. A. Dixon, and R. A. Eades, J. Phys. B 12, 1913 (1979).

[5]D. A. Dixon, R. A. Eades, and D. G. Truhlar, J. Phys. B 12, 2741 (1979).

[6]R. A. Eades, D. G. Truhlar, and D. A. Dixon, Phys. Rev. A 20, 867 (1979).

[7]C. H. Douglas, Jr., D. A. Weil, P. A. Charlier, R. A. Eades, D. G. Truhlar, and D. A. Dixon, in *Chemical Applications of Atomic and Molecular Electrostatic Potentials,* edited by P. Politzer and D. G. Truhlar (Ple-

num, New York, 1981), p. 173.
[8]J. E. Purcell, R. A. Berg, and A. E. S. Green, Phys. Rev. A 2, 107 (1970).
[9]A. E. S. Green, D. E. Rio, and T. Ueda, Phys. Rev. A 24, 3010 (1981).
[10]J. B. Furness and I. E. McCarthy, J. Phys. B 6, 2280 (1973).
[11]I. E. McCarthy, C. J. Noble, B. A. Phillips, and A. D. Turnbull, Phys. Rev. A 15, 2173 (1977).
[12]I. E. McCarthy and M. R. C. McDowell, J. Phys. B 12, 3775 (1979).
[13]See, e.g., F. W. Byron and C. J. Joachain, Phys. Rep. 34C, 234 (1977).
[14]See, e.g., T. Scott and H. S. Taylor, J. Phys. B 12, 3367 (1979).
[15]See, e.g., I. E. McCarthy, B. C. Saha, and A. T. Stelbovics, Phys. Rev. A 23, 145 (1981).
[16]S. M. Valone, D. Thirumalai, and D. G. Truhlar, Int. J. Quantum Chem. Symp. 15, 341 (1981).
[17]R. Lipperheide, Z. Phys. 202, 58 (1967).
[18]K. Onda and D. G. Truhlar, Phys. Rev. A 22, 86 (1980).
[19]M. J. Seaton and L. Steenman-Clark, J. Phys. B 10, 2639 (1977).
[20]R. J. Drachman, J. Phys. B 12, L699 (1979).
[21]D. G. Truhlar and K. Onda, Phys. Lett. 76A, 119 (1980).
[22]D. Thirumalai and D. G. Truhlar, Phys. Rev. A 25, 3058 (1982).
[23]D. Thirumalai and D. G. Truhlar, J. Chem. Phys. 76, 385 (1982).
[24]A. Dalgarno and N. Lynn, Proc. Phys. Soc. London, Ser. A 70, 223 (1957).
[25]R. J. Drachman and A. Temkin, Case Stud. At. Coll. Phys. 2, 399 (1972).
[26]D. G. Thompson, J. Phys. B 4, 468 (1971).
[27]A. E. Garbaty and R. W. LaBahn, Phys. Rev. A 4, 1425 (1971).
[28]K. Blum and P. G. Burke, J. Phys. B 8, L410 (1975).
[29]F. W. Byron, Jr. and C. J. Joachain, Phys. Rev. A 15, 128 (1977).
[30]B. L. Jhanwar, S. P. Khare, and A. Kumar, Jr., J. Phys. B 11, 886 (1978).
[31]A. W. Yau, R. P. McEachran, and A. D. Stauffer, J. Phys. B 11, 2907 (1978).
[32]W. C. Fon and K. A. Berrington, J. Phys. B 14, 323 (1981).
[33]A. Salop and H. H. Nakano, Phys. Rev. A 2, 127 (1970).
[34]S. C. Gupta and J. A. Rees, J. Phys. B 8, 419 (1975).
[35]J. F. Williams and A. Crowe, J. Phys. B 8, 2233 (1975).
[36]R. H. J. Jansen, F. J. deHeer, J. H. Luyken, B. van Wingerden, and J. H. Blaauw, J. Phys. B 9, 185 (1976).
[37]R. D. Dubois and M. E. Rudd, J. Phys. B 9, 2657 (1976).
[38]T. S. Stein, W. E. Kauppila, V. Pol, J. H. Smart, and G. Jesion, Phys. Rev. A 17, 1600 (1978).
[39]J. F. Williams, J. Phys. B 12, 265 (1979).
[40]F. J. deHeer, R. J. H. Jansen, and W. van der Kaay, J. Phys. B 12, 979 (1979).
[41]R. W. Wagenaar and F. J. deHeer, J. Phys. B 13, 3855 (1980).
[42]W. E. Kauppila, J. S. Stein, J. H. Smart, M. S. Dababneh, Y. K. Ho, J. P. Downing, and V. Pol, Phys. Rev. A 24, 725 (1981).
[43]C. J. Kleinman, Y. Hahn, and L. Spruch, Phys. Rev. 165, 53 (1968).
[44]A. Dalgarno, G. W. F. Drake, and G. A. Victor, Phys. Rev. 176, 194 (1968).
[45]*American Institute of Physics Handbook,* edited by D. E. Gray, 3rd ed. (McGraw-Hill, New York, 1972), pp. 7–10.
[46]M. E. Riley and D. G. Truhlar, J. Chem. Phys. 63, 2182 (1975).
[47]T. G. Strand and R. A. Bonham, J. Chem. Phys. 40, 1686 (1964).
[48]F. Calogero, *Variable Phase Approach to Potential Scattering* (Academic, New York, 1967), p. 11.
[49]M. A. Brandt, M. S. thesis, University of Minnesota, Minneapolis, 1975 (unpublished).
[50]E. Clementi, *Tables of Atomic Functions* (IBM Research Laboratories, Calif., 1967), supplement to E. Clementi, IBM J. Res. Dev. 9, 2 (1965).
[51]J. Callaway, Comput. Phys. Commun. 6, 265 (1974).
[52]H. R. J. Walters, J. Phys. B 14, 3499 (1981).
[53]D. F. C. Brewer, W. R. Newell, S. F. W. Harper, and A. C. H. Smith, J. Phys. B 14, L749 (1981).
[54]See document No. PAPS-PLRAA-793-26 for seven pages of appendix containing six tables. Order by PAPS number and journal reference from American Institute of Physics, Physics Auxiliary Publication Service, 335 East 45th Street, New York, N.Y. 10017. The price is $5.00 for a microfiche, or $1.50 for a photocopy. Airmail additional. Make checks payable to the American Institute of Physics.